# Study on Deformation Capacity of R/C Bearing Walls with Rectangular Cross-section Based on Experimental Database

**Masanori Tani & Hiroshi Fukuyama**
*Building Research Institute, Japan*

**Susumu Kono**
*Tokyo Institute of Technology, Japan*

**SUMMARY:**
An experimental database of about 119 R/C bearing wall specimens with rectangular cross-section was made. The accuracy of ultimate flexural and shear capacity estimation methods commonly used in Japan and U.S. was discussed. Based on the database, the statistical analysis was also conducted to assess the influence of the key parameters provided by the codes in Japan and U.S. such as the detail of the boundary elements, the ratio of ultimate flexural capacity to ultimate shear capacity, etc. on the ultimate deformation capacity of the R/C walls.

*Keywords: R/C bearing wall, Experimental database, Ultimate deformation, Ultimate capacity*

## 1. INTRODUCTION

R/C bearing walls have been used as structural members in many countries located at seismic zone because of their high stiffness and capacity. Bearing walls set in a moment resisting frame (walls with boundary columns) have been commonly used in Japan. *AIJ Standard for Structural Calculation of Reinforced Concrete Structures* [AIJ (2010)] was revised in 2010 and permits the use of bearing walls without boundary columns if the requirements are complied. However, these walls are at risk for brittle failure such as compression failure or buckling at wall boundary observed at the 2010 Chile Earthquake as shown in Fig. 1.1 [Tani et al. (2011)]. The research about multi-story bearing walls without boundary columns as structural core walls of high-rise buildings has been conducted recently in Japan and there is some amount of experimental data. In this research, the experimental data of bearing walls without boundary columns in the past literatures was collected. This paper discusses the relationships between deformation capacity and experimental parameters.

## 2. OUTLINE OF DATABASE

The distributions of each experimental parameter and their characteristics are presented in this chapter.

**Figure 1.1.** Damage of multi-story bearing wall without boundary columns at the 2010 Chile Earthquake

The definition of the ultimate deformation is also shown, since it is necessary in the discussion of the deformation capacity.

### 2.1. Distributions of Experimental Parameters

The database consists of experimental data of 119 R/C bearing walls. The specimens had symmetrical dimension and detail, and no openings. The data was obtained from the literatures by Hirosawa et al. (1970), Cardenas et al. (1972), Oesterle et al. (1976), Paulay et al. (1982), Maier et al. (1985), Daniel et al. (1986), Lefas et al. (1990), Lefas et al. (1990), Itadani et al. (1992), Hossein (1994), Cheng et al. (1996), Salonikios et al. (1999), Takeda et al. (1999), Zhang et al. (2000), Hidalgo et al. (2002), Tabata et al. (2003), Furukawa et al. (2003), Thomsen et al. (2004), Greifenhagen et al. (2005), Kimura et al. (2006), Hosoya (2007), Kabeyasawa et al. (2007), Kishimoto et al. (2008), Murakami et al. (2009), Dazio et al. (2009) and Sakamoto et al. (2012). Sixty-three (63) specimens had confined boundary elements (B.E.). The numbers of specimens failed in flexure and shear are 80 and 39, respectively. Ultimate deformation of 82 specimens was obtained. Figures 2.1 and 2.2 show the frequency histograms computed for experimental parameters. Concrete compressive strength ($f'_c$) ranged between 13.8 and 109.1 N/mm$^2$. Sixteen (16) specimens used high strength concrete of $f'_c \geq 60$ N/mm$^2$. The moment-to-shear ratio ($M/(QD)$) ranged between 0.35 and 5.00. No specimen with $M/(QD)$ greater than 1.5 failed in shear. The length-to-thickness ratio ($D/t_w$) ranged between 5.3 and 30.0, and web thickness ($t_w$) ranged between 60 and 160 mm. The axial load ratio ($N/(A_g\sigma_B)$) varied between 0.00 and 0.35. Fifty (50) specimens were tested under no axial load. The vertical web reinforcement ratio ($p_{wv}$) ranged between 0 and 0.0264 and the horizontal web reinforcement ratio ($p_{wh}$) ranged between 0 and 0.0172. Six specimens had no web reinforcement. The ratio of boundary

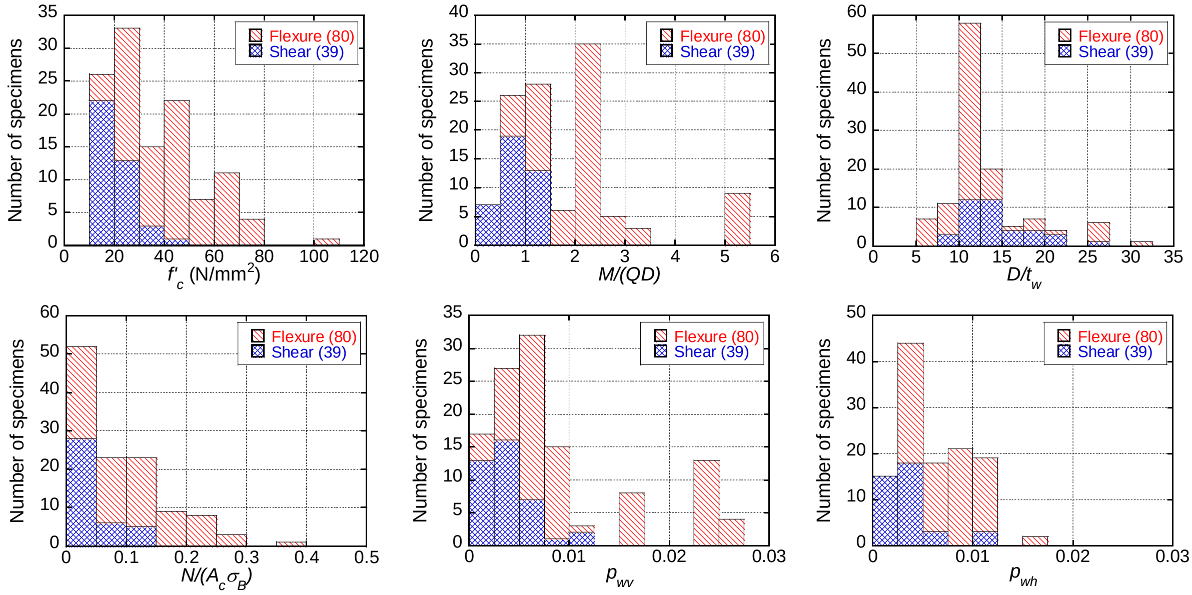


**Figure 2.1.** Histograms of experimental parameters of all specimens (119 specimens)

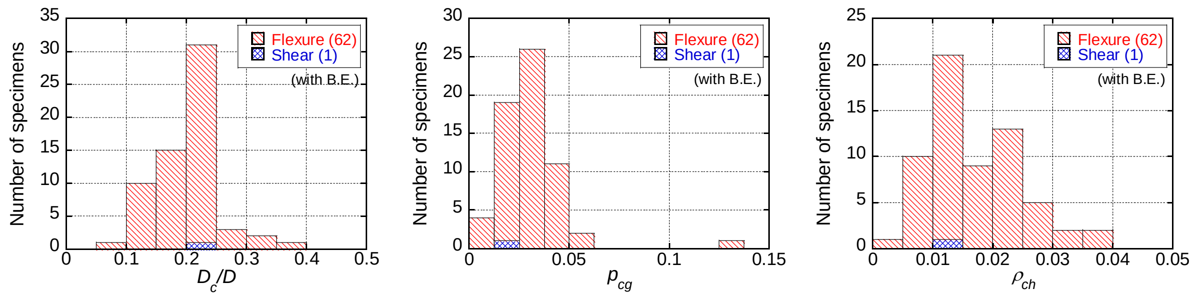


**Figure 2.2.** Histograms of experimental parameters of specimens with boundary elements (63specimens)

element depth to wall length ($D_c/D$) ranged between 0.07 and 0.38. The vertical reinforcement ratio of the boundary element ($p_{cg}$) ranged between 0.008 and 0.126. The volumetric ratio of transverse reinforcement of the boundary element ($\rho_{ch}$) ranged between 0.003 and 0.039.

### 2.2. Definition of Ultimate Deformation

Although various definitions of ultimate deformation exist, the deformation where the capacity dropped to 80 % of the maximum capacity in the post-peak region was defined as the ultimate deformation in this paper. In the case there was no description about the ultimate deformation in a literature, the values were read from the diagrams of the relationship between load (or moment) and displacement according to the following rules;

- If the 80 % capacity appeared on the skeleton, the ultimate deformation was defined as the deformation at that time.
- If a specimen had over the 80 % capacity at a certain loading cycle and the capacity did not reach to the 80 % capacity at the next loading cycle with larger deformation, the deformation at the 80 % capacity on the line connected the maximum deformation point in the certain loading cycle and the maximum capacity point in the next loading cycle is defined as the ultimate deformation.
- If a specimen had more than 80 % capacity at the first cycle and the capacity did not reach to the 80 % capacity at the second cycle during the loading cycle of the same deformation, the maximum deformation at the first cycle is defined as the ultimate deformation.
- In principle, ultimate deformation is the average value in the positive and negative loading. In the case the capacity fell below 80 % capacity in the positive loading before the maximum capacity revealed in the negative loading, the ultimate deformation is defined by only the positive loading.

## 3. ESTIMATION OF ULTIMATE CAPACITY

The accuracy of the current equations used for estimating ultimate flexural and shear capacity of bearing walls are presented in this chapter. Discussions about the prediction of failure mode are also conducted.

### 3.1. Ultimate Flexural Capacity

The accuracy of the evaluation method of ultimate flexural capacity is discussed. The target specimens are 80 specimens failed in flexure. Equation 3.1 is a simplified equation of the ultimate flexural capacity shown in *the Commentary of Japanese Building Code for Structural Safety*. This equation assumes yielding of all vertical reinforcement in the wall boundary area and web. The applicable axial load of Eqn. 3.1 is not provided because the axial load applied on the actual bearing walls is not too large in general.

$$ {}_{c}Q_{mu} = \frac{a_t f_y l_w + 0.5 a_w f_{wy} l_w + 0.5 N l_w}{a} \tag{3.1} $$

where, $a_t$, $f_y$: area and yield stress of vertical reinforcement in the wall boundary area, $a_w$, $f_{wy}$: area and yield stress of vertical web reinforcement, $N$: axial load, $l_w$: length between the centers of boundary columns (0.9$D$ for rectangular cross-section), $D$: wall length.

The definition of "wall boundary area" of $a_t$ and $f_y$ is not specified clearly in the literature. Therefore, $a_t$ was evaluated as follows in this paper. The cross-sectional area of vertical reinforcement in the boundary element was defined as $a_t$ of specimens with boundary elements. The cross-sectional area of vertical reinforcement within 0.1$D$ from the wall edge was defined as $a_t$ of specimens without boundary elements.

The experimental maximum capacity of flexural-failure specimens is plotted against the calculated flexural capacity in Fig. 3.1. Circular and triangular dots indicate the result of specimens with and without boundary elements, respectively. Solid dots are for the specimens with web reinforcement ratio less than 0.0025. The statistics of the ratio of the ultimate flexural capacity estimated by Eqn. 3.1 to the experimental maximum capacity is also summarized in Table 3.1. Ratios of experimental capacity to calculated capacity by Eqn. 3.1 for specimens with boundary elements and over 0.0025 web reinforcement ranged between 0.73 and 1.26. The mean value and the coefficient of variable were 0.97 and 0.12, respectively. The number of the specimens whose experimental capacity was estimated within the error of 20 % was 52. Ratios of experimental capacity to calculated flexural capacity for specimens without boundary elements and over 0.0025 web reinforcement ranged between 0.68 and 1.34. The mean value and the coefficient of variable were 0.98 and 0.19, respectively. The number of the specimens whose experimental capacity was estimated within the error of 20 % was 12. The tendency that the prediction accuracy for the specimens with boundary elements was better than that for the specimens without boundary elements was observed. Although Eqn. 3.1 has good prediction accuracy considering it is a simplified equation, many specimens were overestimated of their maximum capacity. Relationship between ${}_eQ_u/{}_cQ_{mu}$ and axial load ratio is illustrated in Fig. 3.2. As shown in Fig. 3.2, almost all the flexural capacity of specimens with axial load ratio larger than 0.10 was overestimated. Because the compression failure of concrete becomes more dominant as axial load becomes larger, the specimens with large axial load ratio are thought to be out of the application of Eqn. 3.1 which assumes yielding of tensile reinforcement as described above. Therefore, it is thought that plane section analysis is needed in calculation of ultimate flexural capacity for the specimens with axial load ratio greater than 0.10.

### 3.2. Ultimate Shear Capacity

The prediction accuracy of the equations of ultimate shear capacity used in Japan and U.S. is discussed. The target is 39 specimens which failed in shear (with boundary elements: 1, without boundary elements: 38). Equation 3.2 is an empirical equation of ultimate shear capacity provided in *the Commentary of Japanese Building Code for Structural Safety*. Equation 3.2 is thought to give the

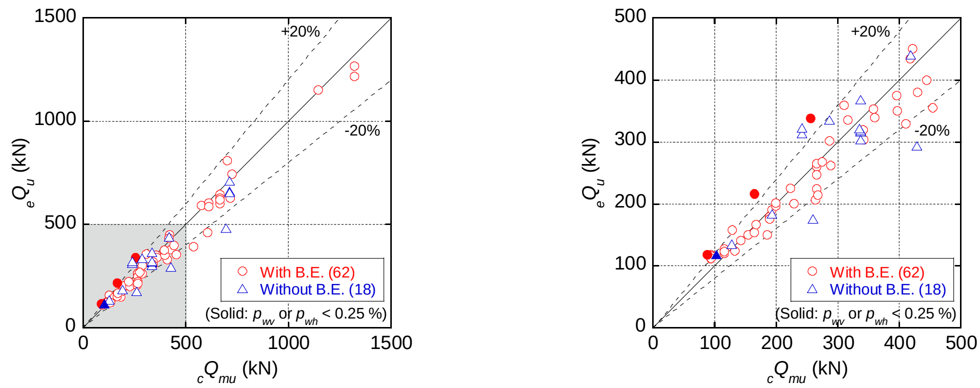


(a) All specimens (b) Close-up of (a)

**Figure 3.1.** Comparison between the calculated flexural capacity and experimental maximum capacity

**Table 3.1.** Statistics of ${}_eQ_u/{}_cQ_{mu}$ of specimens which failed in flexure

| | With B.E. | Without B.E. |
|---|---|---|
| Number | 59 (3) | 17 (1) |
| Mean | 0.97 (1.33) | 0.98 (1.14) |
| Max. | 1.26 (1.35) | 1.34 (-) |
| Min. | 0.73 (1.32) | 0.68 (-) |
| C.V. | 0.12 (0.02) | 0.19 (-) |
| $R_{20\%}$ | 0.88 (0.00) | 0.71 (1.00) |

*The values of specimens with web reinforcement ratio smaller than 0.0025 were shown in parentheses.

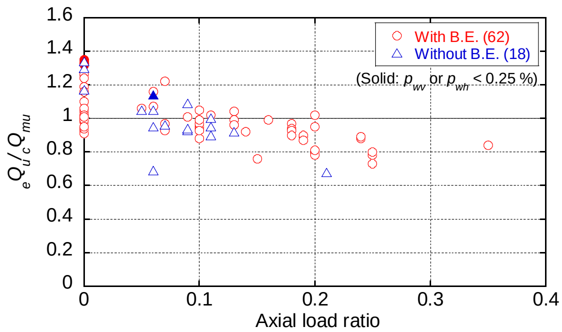


**Figure 3.2**. Variation of ${}_eQ_u/{}_cQ_{mu}$ with axial load ratio

mean value of shear capacity of bearing walls and the most commonly used in Japan. Equation 3.2 has no requirement of web reinforcement ratio, although the minimum spacing and diameter of web reinforcement are required. Equation 3.3 is provided in Section 21.9.4 of ACI 318-11 for calculation of shear strength of special structural walls. ACI 318-11 requires that vertical web reinforcement ratio shall not be less than horizontal reinforcement ratio if $h_w/D$ does not exceed 2.0. ACI 318-11 also has a requirement that web reinforcement ratio for structural walls shall not be less than 0.0025.

$$ {}_{c}Q_{su1} = \left\{ \frac{0.068 p_{te}^{\;0.23}\left(f'_c + 18\right)}{\sqrt{M/(QD) + 0.12}} + 0.85\sqrt{f_{wh}\, p_{wh}} + 0.1\sigma_0 \right\} t_e\, j \tag{3.2} $$

$$ {}_{c}Q_{su2} = A_w\left(\alpha_c \sqrt{f'_c} + p_{wh} f_{wh}\right) \le 0.83\sqrt{f'_c}\, A_w \tag{3.3} $$

where, $p_{te}$: equivalent tensile reinforcement ratio (%) ($=100a_t/t_e d$), $t_e$: equivalent wall thickness, $d$: effective length of wall ($=0.95D$), $M/(QD)$: moment-to-shear ratio ($1 \le M/(QD) \le 3$), $f_{wh}$: yield strength of horizontal web reinforcement, $\sigma_0$: average axial stress to gross cross-sectional area, $j$: length of rebar arm ($=7/8d$), $\alpha_c$: a function of aspect ratio (equal to 0.25 for $h_w/D \le 1.5$, 0.17 for $h_w/D \ge 2.0$, and varies linearly between 0.25 and 0.17 for $h_w/D$ between 1.5 and 2.0), $h_w$: clear height of wall, $A_w$: gross cross-sectional area.

Figure 3.3 illustrates the comparison between calculated ultimate shear capacity and experimental maximum capacity of 39 specimens which failed in shear. Circular dots and triangular dots indicate the result of specimens with and without boundary elements, respectively. Open dots are for ACI 318-compliant specimens (the web reinforcement requirements, $p_{wv} \ge 0.0025$, $p_{wh} \ge 0.0025$ and $p_{wv} \ge p_{wh}$, are complied). The statistics of the ratio of the ultimate shear capacity estimated by Eqns. 3.2 and 3.3 to the experimental maximum capacity of shear-failure specimens is summarized in Table 3.2. Discussion about the specimen with boundary elements is omitted because there was only one

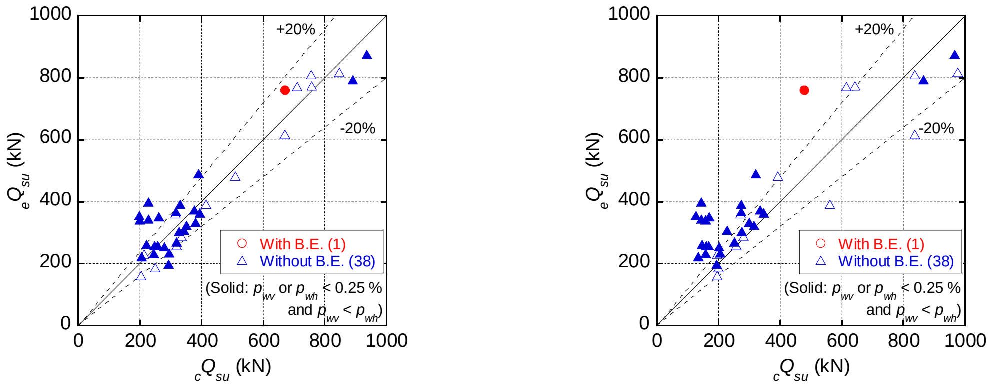


(a) Equation 3.2　　(b) Equation 3.3

**Figure 3.3.** Comparison between calculated shear capacity and experimental maximum capacity

**Table 3.2.** Statistics of ${}_{e}Q_u/{}_{c}Q_{su}$ by Eqns. 3.2 and 3.3 of specimens failed in shear

| | With boundary elements | | Without boundary elements | |
|---|---|---|---|---|
| | Eqn. 3.2 | Eqn. 3.3 | Eqn. 3.2 | Eqn. 3.3 |
| Number | 0 (1) | | 13 (25) | |
| Mean | - (1.13) | - (1.59) | 0.95 (1.10) | 1.02 (1.50) |
| Max. | - (-) | - (-) | 1.15 (1.79) | 1.33 (2.80) |
| Min. | - (-) | - (-) | 0.75 (0.67) | 0.70 (0.91) |
| C.V. | - (-) | - (-) | 0.13 (0.28) | 0.20 (0.36) |
| $R_{20\%}$ | - (1.00) | - (0.00) | 0.85 (0.68) | 0.64 (0.40) |

*The values of specimens which did not comply with the ACI requirements were shown in parentheses.

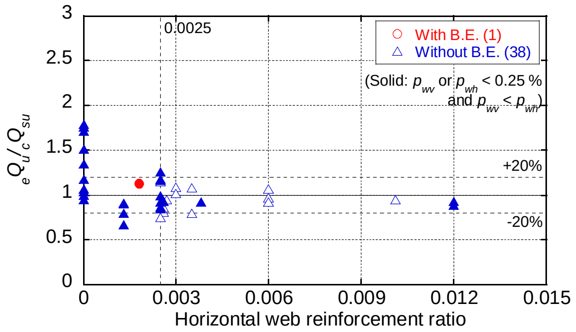


(a) Equation 3.2 (b) Equation 3.3

**Figure 3.4.** Variation of $_eQ_u/_cQ_{su}$ with horizontal web reinforcement ratio

specimen. Equations 3.2 and 3.3 were able to predict the shear capacity of the specimens without boundary elements compliant with the ACI requirements in a good accuracy. For the specimens without boundary elements and incompliance with the ACI requirements, although some scatter was observed in the estimation by Eqn. 3.2, almost the mean estimation was obtained. Calculated results by Eqn. 3.3 exhibited larger scatter and considerably underestimation. Figure 3.4 presents the variation of $_eQ_u/_cQ_{su}$ with horizontal web reinforcement ratio. Equation 3.2 estimated the ultimate shear capacity of the specimens with horizontal web reinforcement ratio smaller than 0.0025 in moderate accuracy, though the calculated results of specimens had no horizontal web reinforcement varied widely. On the other hand, Eqn. 3.3 considerably underestimated the capacity of these specimens. It is noted that the accuracy of Eqn. 3.3 is sensitive to the horizontal web reinforcement ratio.

### 3.3. Prediction of Failure Mode

The ratios of experimental maximum capacity to calculated flexural capacity are plotted against the ratios of calculated shear capacity to calculated flexural capacity in Fig. 3.5. Ultimate flexure and shear capacity are obtained by Eqns. 3.1 and 3.2. The ACI 318-incompliant specimens were excluded and the target in this section is 77 specimens. Circular dots and triangular dots indicate the result of specimens with and without boundary elements, respectively. Open and solid dots are for flexural-failure and shear-failure specimens, respectively. As seen in Fig. 3.5, only one specimen with $_cQ_{su}/_cQ_{mu}$ larger than 1.0 failed in shear. From the point of view that shear failure has to be prevented, the failure mode prediction by Eqns. 3.1 and 3.2 is thought to be useful.

## 4. DISCUSSIONS ON ULTIMATE DEFORMATION

The relationship between the indexes about deformation capacity estimation provided by the Japanese standard and the ACI code and experimentally obtained ultimate deformation is discussed in this chapter. The target is 51 specimens of ACI 318-compliant specimens whose ultimate deformation

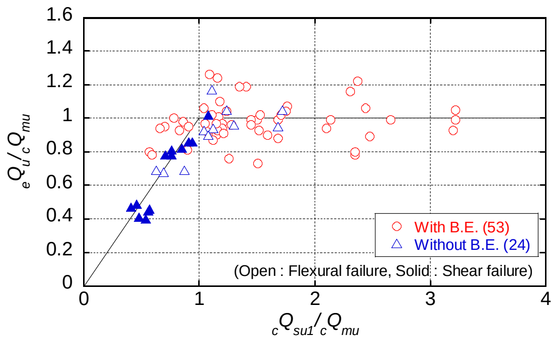


**Figure 3.5.** Variation of $_eQ_u/_cQ_{mu}$ with $_cQ_{su1}/_cQ_{mu}$

capacity was obtained.

### 4.1 Parameters of Deformation Capacity in Japanese Standards

The ratio $\tau_f/\sigma_B$ is to be used as an index of deformation capacity evaluation of bearing walls in the Japanese structural design. Index $\tau_f$ is the ultimate flexural capacity normalized by $A_w$. A bearing wall with small $\tau_f/\sigma_B$ is ranked as a member with high deformation capacity proved not to show brittle failure such as shear failure. There are four ductility ranks of bearing walls, WA through WD in descending order according to the deformation capacity. Although the value of deformation capacity corresponding to each ductility rank is not specified, some recent researches remark that WA members have the deformation capacity as ultimate drift angle exceeds 0.015. When the calculation of horizontal load-carrying capacity in the structural design, the more high-ranked members exist, the more required horizontal load-carrying capacity becomes. Figure 4.1 indicates the variation of the experimental ultimate deformation with $\tau_f/\sigma_B$. Criteria of the ductility rank are also shown in Fig. 4.1. The concept of this evaluation method is correct to some extent because the trend that $R_u$ becomes smaller as $\tau_f/\sigma_B$ increases was observed as seen in Fig. 4.1. The plots of specimens with $\tau_f/\sigma_B$ less than 0.15 are scattered. There are some specimens with small deformation capacity as $R_u$ was around 0.01, nevertheless $\tau_f/\sigma_B$ was less than 0.1 and ${}_cQ_{su}/{}_cQ_{mu}$ also exceeded 1.25. The characteristics of these specimens are expressed as follows. (a) Specimens with small axial load ratio and web reinforcement ratio failed in sliding shear after flexural yielding [Salonikios et al. (1999)]. (b) Specimens under relatively high axial load showed compression failure [Tabata et al. (2003)]. (c) Ductility of vertical reinforcement was small and the rupture of them was observed [Dazio et al. (2009)]. In order to evaluate the deformation capacity adequately, for example, the requirements about the minimum amount of vertical reinforcement in web and boundary elements and transverse reinforcement in boundary elements is necessary. The requirement about the maximum axial load is also needed.

*Seismic evaluation of existing reinforced concrete buildings* (2004) provides a simplified evaluation method of deformation capacity of bearing walls using the ratio of ultimate shear capacity to ultimate flexural capacity, ${}_cQ_{su}/{}_cQ_{mu}$. Specifically, ductility index $F$ equals to 1.0 for ${}_cQ_{su}/{}_cQ_{mu} \leq 1.0$, 1.5 for ${}_cQ_{su}/{}_cQ_{mu} \geq 1.3$ and varies linearly for $1.0 \leq {}_cQ_{su}/{}_cQ_{mu} \leq 1.3$ for walls with rectangular cross-section. Ductility index $F$ = 1.0, 1.27 and 1.5 correspond to drift angle $R$ = 1/250, 1/150 and 1/125, respectively. Ultimate deformation is plotted against ${}_cQ_{su}/{}_cQ_{mu}$ in Fig. 4.2. The deformation capacity corresponds to ductility index is also shown in Fig. 4.2. Ductility index estimates the lower values of ultimate deformation. It is hard to say that ductility index can predict the ultimate deformation capacity adequately because the upper drift angle by ductility index equals to 1/125. Because both methods assume shear dominated failure mode, they are not applicable to multi-story bearing walls with large moment-to-span ratio which show high ductility.

### 4.2 Parameters of Deformation Capacity in ACI Code

Section 21.9.6 of ACI318-11 provides some requirements for boundary elements of special structural walls. In more detail, there are criteria of the need for special boundary elements and the requirements

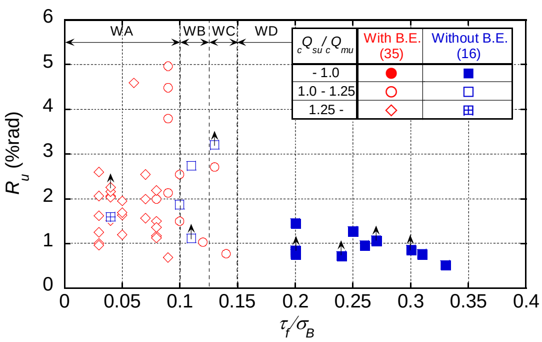


**Figure 4.1.** Variation of $R_u$ with $\tau_f/\sigma_B$

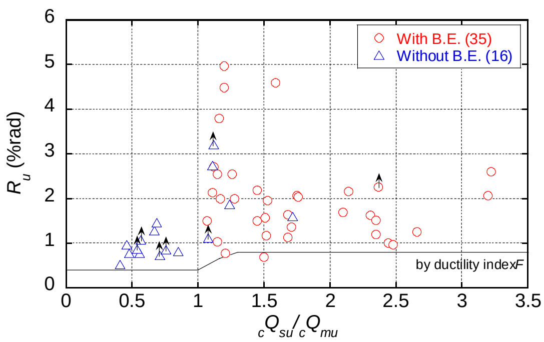


**Figure 4.2.** Variation of $R_u$ with ${}_cQ_{su}/{}_cQ_{mu}$

about length of the special boundary element and amount and spacing of the transverse reinforcement in the special boundary element. In this section, the relationship between these requirement and deformation capacity obtained in the experiment is discussed.

Section 21.9.6.2 (a) requires special boundary elements for special structural walls whose neutral axis depth $c$ exceeds $D/600(\delta_d/h_w)$. However, neutral axis depth is to be obtained by strain compatibility analysis, it was derived abbreviately using the ACI concrete equivalent stress block and the assumption that vertical reinforcement in web and boundary elements yielded as Eqn. 4.1. The need of special boundary element is evaluated by assuming $\delta_u/h_w$ equals 0.015 in this paper. However, there were four specimens not required special boundary elements, they complied with the requirements by Section 21.9.6.5. The minimum length of special boundary element $D_{c.ACI}$ is required in Section 21.9.6.4 (a) as shown in Eqn. 4.2. The maximum spacing and the minimum amount of special boundary element transverse reinforcement are required by Section 21.9.6.4 (c) as shown in Eqns. 4.3 through 4.5. Section 21.6.4.2 requires the spacing of crossties of legs of rectilinear hoops, $h_x$, shall not exceed 350 mm.

$$c = \frac{N + \sum a_t f_y}{0.85\beta f'_c\, t}, \quad D_{c.ACI} = \max(c - 0.1D, \quad c/2) \qquad (4.1), (4.2)$$

$$s_{ACI} = \min\left( \min\left( \frac{b_c}{3}, \quad \frac{D_c}{3} \right), \quad 6d_{cv}, \quad 100 \le 100 + \left( \frac{350 - h_x}{3} \right) \le 150 \right) \qquad (4.3)$$

$$\rho_{s.ACI} = \max\left( \frac{0.12 f'_c}{f_{ch}}, \quad 0.45\left( \frac{A_w}{A_{ch}} - 1 \right) \frac{f'_c}{f_{ch}} \right), \quad A_{sh.ACI} = 0.09 \frac{s b_c f'_c}{f_{ch}} \qquad (4.4), (4.5)$$

where, $s_{ACI}$: the minimum spacing of transverse reinforcement required by Section 21.6.4.3, $b_c$, $D_c$: width and depth of the boundary element, $d_{cv}$: diameter of the smallest vertical reinforcement in the boundary element, $\rho_{s.ACI}$: the minimum volumetric ratio of spiral or circular hoop reinforcement in the boundary element required by Section 21.6.4.4 (a), $f_{ch}$: yield stress of spiral or circular hoop reinforcement in the boundary element (not exceed 700 $N/mm^2$), $A_{ch}$: area measured to the outside edges of transverse reinforcement, $A_{sh.ACI}$: the minimum total area of rectangular hoop reinforcement required by Section 21.6.4.4 (b), $s$: spacing of transverse reinforcement.

The target in this section is 35 specimens with boundary elements and web reinforcement compliant with the ACI 318 requirements. Only three specimens (NC40 by Sakamoto et al. (2011) and LSW1 and LSW3 by Salonikios (1999)) complied with all the requirements of special boundary elements described above. NC40 failed in compression at the wall edge, but exhibited good deformation capacity as ultimate drift angle exceeded 0.02. LSW1 and LSW3 failed in sliding shear after flexural yielding and ultimate drift angle remained around 0.01.

The discussion on the effect of the parameters used in the ACI requirements to the deformation capacity of wall is conducted. Figures 4.3 through 4.6 indicate the relationships between the ultimate deformation and the ratio of the experimental value to the required value of each parameter obtained by Eqns. 4.2 through 4.5. As mentioned above, the requirements of volumetric ratio and total area of transverse reinforcement are provided in ACI 318. The requirement of total area is much tighter than that of volumetric ratio as shown in Figs. 4.3 and 4.4. Still, many specimens incompliant with the amount requirement exhibited sufficient deformation capacity. As with the depth of boundary element in Fig. 4.5, it is difficult to find the relationship between $D_c/D$ and deformation capacity. In Fig. 4.6, the trend that deformation capacity decreases with increasing of transverse reinforcement spacing is observed except for the specimens failed in sliding shear or incompliant with the other requirements. Although it may be premature conclusion because there are not enough specimens, these results indicate that spacing of transverse reinforcement has the most significant influence on the deformation capacity.

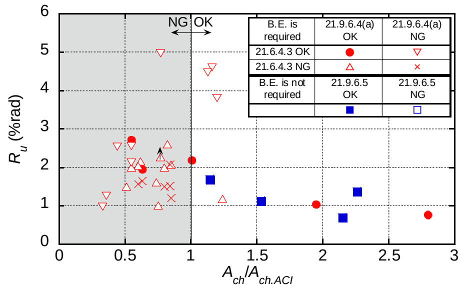


**Figure 4.3.** Variation of $R_u$ with $A_{ch}/A_{ch.ACI}$

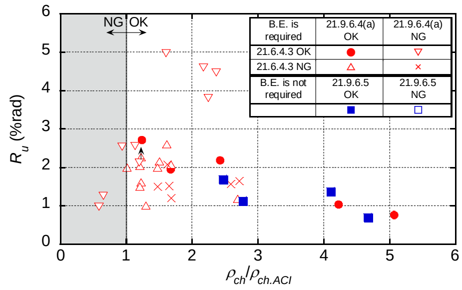


**Figure 4.4.** Variation of $R_u$ with $\rho_{ch}/\rho_{ch.ACI}$

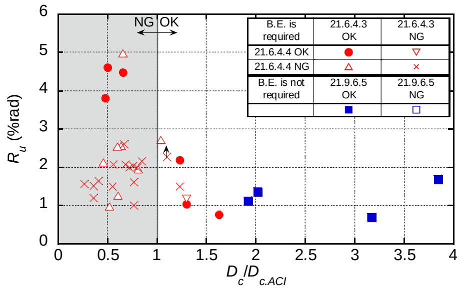


**Figure 4.5.** Variation of $R_u$ with $D_c/D_{c.ACI}$

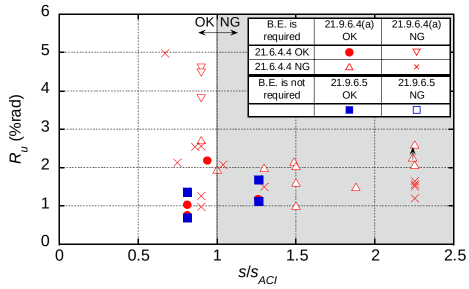


**Figure 4.6.** Variation of $R_u$ with $s/s_{ACI}$

## 5. CONCLUSIONS

An experimental database of 119 R/C bearing walls with rectangular cross-section was made to discuss ultimate capacity and ultimate deformation. The following conclusions are obtained.

- The Japanese simplified equation for ultimate flexural capacity estimation was able to predict the experimental maximum capacity of flexural-failure specimens accurately. But, almost all the flexural capacity of specimens with axial load ratio larger than 0.10 was overestimated.
- The Japanese equation for ultimate shear capacity estimation gave the mean estimation of the experimental maximum capacity of shear-failure specimens in a good accuracy, although some scatter was observed for the specimens with small web reinforcement ratio. The ACI 318-11 equation was sensitive to web reinforcement ratio and gave significant underestimation for the specimens with small web reinforcement ratio.
- The relevant of the evaluation indexes in Japan, $\tau_f/\sigma_B$ and ${}_cQ_{su}/{}_cQ_{mu}$ to deformation capacity was discussed. The concept about $\tau_f/\sigma_B$ was found to be correct because the trend that $R_u$ becomes smaller as $\tau_f/\sigma_B$ increases was observed, though the plots of specimens with $\tau_f/\sigma_B$ less than 0.15 were scattered. The index ${}_cQ_{su}/{}_cQ_{mu}$ estimated the lower values of ultimate deformation.
- Discussion on the relationship between the ACI requirements of the special boundary element and deformation capacity. The spacing of transverse reinforcement has the most significant influence on the deformation capacity, of all the requirements about the amount and spacing of transverse reinforcement and the depth of boundary elements.

## REFERENCES


Hirosawa, M. and Goto, T. (1970). Experimental study on ductile monolithic reinforced concrete wall. *Annual Report of Building Research Institute*. 65-79. (in Japanese)

Cardenas, A. E. and Magura, D. D. (1972). Strength of high-rise shear walls - rectangular cross section. *ACI publication SP-36*. 119-150.

Oesterle, R. G., et al. (1976). Earthquake resistant structural walls - Tests of isolated walls. *Report to the National Science Foundation. Construction Technology Laboratories*. Portland Cement Association.

Paulay, T., et al. (1982). Ductility in earthquake resisting squat shearwalls. *ACI Journal*. **79:4**, 257-269.
Maier, J. and Thürlimann, B. (1985). Bruchversuche an Stahlbetonscheiben. *Institut für Baustatik und Konstruktion Bericht*. ETH. 8003-1. (in German)
Daniel, J. I., et al. (1986). Openings in earthquake-resistant structural walls. *Journal of Structural Engineering*. ASCE. **112:7**, 1660-1676.
Lefas, I. D., et al. (1990). Behavior of reinforced concrete structural walls: strength, deformation characteristics, and failure mechanism. *ACI Structural Journal*. **87:1**, 23-31.
Lefas, I. D. and Kotsovos, M. D. (1990). Strength and deformation characteristics of reinforced concrete walls under load reversals. *ACI Structural Journal*. **87:6**, 716-726.
Itadani, H., et al. (1992). Experimental study on strength of reinforced concrete wall (Part 1 and 2). *Summaries of Technical Papers of Annual Meeting*. AIJ. **C**, 353-356. (in Japanese)
Hossein, M. D. (1994). Behaviour and design of earthquake resistant low-rise shear walls. Department of Civil Engineering. University of Ottawa.
Cheng, F. Y. and Yang, J. S. (1996). Hysteresis rules and design parameter assessment of RC low-rise shear walls and buildings with openings. Department of Civil Engineering. University of Missouri-Rolla.
Salonikios, T. N., et al. (1999). Cyclic load behavior of low-slenderness reinforced concrete walls: Design basis and test results. *ACI Structural Journal*. **96:4**, 649-660.
Takeda, T., et al. (1999). Experimental study on flexural behavior of high-strength reinforced concrete shear walls (Part 1 and 2). *Summaries of Technical Papers of Annual Meeting*. AIJ. **C-2**, 371-374. (in Japanese)
Zhang, Y. and Wang, Z. (2000). Seismic behavior of reinforced concrete shear walls subjected to high axial loading. *ACI Structural Journal*. **97:5**, 739–750.
Hidalgo, P. A., et al. (2002). Seismic behavior of squat reinforced concrete shear walls. *Earthquake Spectra*. **18:2**, 287-308.
Tabata, T., et al. (2003). Experimental study on strucural performance of R/C walls under high flexural stress. *Proceedings of the Japan Concrete Institute*. **25:2**, 625-630. (in Japanese)
Furukawa, J., et al. (2003). Experimental study on flexural behavior of reinforced concrete shear walls. *Summaries of Technical Papers of Annual Meeting*. AIJ. **C-2**, 317-320. (in Japanese)
Thomsen IV, J. H. and Wallace, J.W. (2004). Displacement-based design of slender reinforced concrete structural walls-experimental verification. *Journal of Structural Engineering* **130:4**, 618-630.
The Japan Building Disaster Prevention Association (2004). *Standard for seismic evaluation of existing reinforced concrete buildings, 2001*.
Greifenhagen, C. and Lestuzzi, P. (2005). Static cyclic tests on lightly reinforced concrete shear walls. *Engineering Structures*. **27**. 1703-1712.
Kimura, H. and Ishikawa, Y. (2006). Study on structural performance of rectangular cross section R/C walls. *Proceedings of the Japan Concrete Institute*. **28:2**, 469-474. (in Japanese)
Hosoya, H. (2007). Structural performance of R/C rectangular section core walls. *Proceedings of the Japan Concrete Institute*. **29:3**, 313-318. (in Japanese)
Kabeyasawa, T., et al. (2007). Experimental study on shape and reinforcing of RC walls (Part 1). *Summaries of Technical Papers of Annual Meeting*. AIJ. **C-2**, 461-462. (in Japanese)
Kishimoto, T., et al. (2008). Study on structural performance of R/C rectangular section core walls (Part 3 and 4). *Summaries of Technical Papers of Annual Meeting*. AIJ. **C-2**, 355-358. (in Japanese)
Murakami, H., et al. (2009). Experimental study on structural performance of RC multi-story shear wall (Part 1 and 2). *Summaries of Technical Papers of Annual Meeting*. AIJ. **C-2**, 425-428 (in Japanese)
Dazio, A., et al. (2009). Quasi-static cyclic tests and plastic hinge analysis of RC structural walls. *Engineering Structures*. **31**. 1556-1571.
Architectural Institute of Japan (2010). *AIJ Standard for Structural Calculation of Reinforced Concrete Structures*. (in Japanese)
Tani, M., et al. (2011). Building damage in 2010 Chile Offshore Maule Earthquake (Part 1). *Summaries of Technical Papers of Annual Meeting*. AIJ. **C-2**, 907-908. (in Japanese)
ACI Committee 318 (2011). *Building Code Requirements for Structural Concrete (ACI 318-11) and Commentary*.
Sakamoto, K., et al. (2012). Effect of boundary columns and amount of boundary elements on ultimate flexural deformation capacity of RC bearing walls. *Proceedings of the Japan Concrete Institute*. **34**. (in Japanese)